

July 14, 2005  
hep-lat/0507016

# R-symmetry in the Q-exact (2,2) 2d lattice Wess-Zumino model

Joel Giedt\*

*University of Toronto, Department of Physics  
60 St. George St., Toronto ON M5S 1A7 Canada*

## Abstract

In this article we explore the R-symmetry of the (2,2) 2d Wess-Zumino model. We study whether or not this symmetry is approximately realized in the Q-exact lattice version of this theory. Our study is nonperturbative: it relies on Monte Carlo simulations with dynamical fermions. Irrelevant operators in the lattice action explicitly break the R-symmetry. In spite of this, it is found to be a symmetry of the effective potential. We find nonperturbative evidence that the nonrenormalization theorem of the continuum theory is recovered in the continuum limit; e.g., there is no additive mass renormalization. In our simulations we find that Fourier acceleration of the hybrid Monte Carlo algorithm allows us to avoid difficulties with critical slowing-down.

---

\*giedt@physics.utoronto.ca

# 1 Motivation

The continuum (2,2) 2d Wess-Zumino (2dWZ) model (obtained from a dimensional reduction of the 4d Wess-Zumino model [1]) is supposed to provide a Landau-Ginzburg description of the minimal discrete series of  $\mathcal{N} = 2$  superconformal field theories [2]. In the present article, we examine an important aspect of the simplest of these models—the one with a cubic superpotential—in the context of class of lattice actions that have an exact lattice supersymmetry. These lattice actions were first formulated in [3, 4] using *Nicolai map* [5] methods, relying on earlier Hamiltonian [6] and continuum [7] studies that also utilized the Nicolai map. Detailed studies of the spacetime lattice system were performed in [8] by stochastic quantization methods and in [9] by the Monte Carlo simulation approach.

Once auxiliary fields are introduced, the lattice action takes a Q-exact form:  $S = QX$ , as was emphasized in topological interpretation of [10] and the lattice superfield approach of [11]. Here  $Q$  is a lattice supercharge with derivatives realized through discrete difference operators; with respect to a discrete approximation of the continuum theory superalgebra,  $Q^2 = 0$  is a nilpotent subalgebra. Because  $S$  is Q-exact, the action is trivially invariant with respect to this lattice supersymmetry:  $QS = Q^2X = 0$ .

In the massive continuum theory, as will be shown below, there is an exact  $Z_2(R)$  symmetry. It is an *R-symmetry*, meaning it does not commute with the supercharges. This symmetry is spontaneously broken at infinite volume. In the massless case, i.e., in the critical domain, the classical R-symmetry is enlarged to  $U(1)_R$ . It cannot be spontaneously broken since it is a continuous symmetry in 2d [12]. If the lattice theory has the correct continuum limit, it should reproduce these features. On the other hand, these R-symmetries are only approximate in the Q-exact lattice action; the symmetry is explicitly broken by the Wilson mass term that is used to lift doublers.<sup>1</sup>

It has been shown in [11] that the continuum limit of the lattice perturbation series is identical to that of the continuum theory, due to cancellations that follow from  $Q^2 = 0$ . Thus, the Q-exact spacetime lattice has behavior that is similar to what was found on the  $Q, Q^\dagger$ -preserving spatial lattice in [3]. However, it was also shown in [11] that the most general continuum effective action that is consistent with the symmetries of the bare lattice action is not the (2,2) 2d Wess-Zumino model. This raises the question of whether or not the good behavior of perturbation theory persists at a nonperturbative level. The Monte Carlo simulation results of Catterall et al. give hope that the desired continuum limit is obtained beyond perturbation theory [9]. If so, this would be one of the few examples of a supersymmetric field theory that can be latticized and studied nonperturbatively by Monte Carlo simulation without the need for fine-tuning of counterterms.

Though not directly related, we pause to mention that lattice super-Yang-Mills

---

<sup>1</sup>This is directly related to the breaking of the so-called  $U(1)_V$  symmetry, that was pointed out in [11].

theories exist that do not require fine-tuning of counterterms [13], at least within perturbation theory. However, in some of those cases, it is known that the fermion determinant has a complex phase that depends on the boson configuration [14]. The complex phase poses a severe difficulty for Monte Carlo simulations of those systems [15].

If we can show that features of the continuum theory associated with the R-symmetry are recovered in the continuum limit, it provides further evidence that the correct theory is obtained. The symmetry that we study persists in the infrared effective theory in a strongly coupled regime. Thus, we are testing aspects of the lattice theory that lie beyond the reach of perturbation theory.

We now summarize the rest of this article:

- In Section 2, we briefly describe the continuum theory that the lattice model is supposed to define. We discuss both the general (2,2) 2d Wess-Zumino model, and the specific case that we select for further study: the model with a cubic superpotential. In that case, we show that there is a classical  $Z_2(R)$  symmetry. We explain that it must be spontaneously broken, according to a well-known theorem for 2d field theories with a stable potential.
- In Section 3, the lattice action is described. Symmetry aspects of the action are emphasized. In particular, we show that when doublers are lifted by a supersymmetric version of the Wilson mass term, the  $Z_2(R)$  is explicitly broken. However, it is an approximate classical symmetry for the long wavelength modes.
- In Section 4, observables are defined that are used in our study of the critical domain. Basic data regarding their behavior is briefly described. Degenerate minima of the effective potential lead to tunneling in the simulations at finite volume. We describe how observables are chosen that are insensitive to this finite volume effect. Next the  $Z_2(R)$  symmetry is examined in our simulations. We find that the effective potential exhibits this symmetry to a very good approximation. We show that as the volume is increased, spontaneous symmetry-breaking of  $Z_2(R)$  is clearly evident. Finally, we demonstrate that the  $U(1)_R$  symmetry of the effective potential is recovered in the critical domain. We find evidence that the nonrenormalization theorems of the continuum theory hold to a good approximation in the limit of small lattice spacing.
- In Section 5, we conclude with an interpretation of our simulation results. We also outline future directions for research in this lattice system.
- In Appendix A, the simulation methods are outlined. We describe the extent to which we were able to overcome critical slowing-down using Fourier acceleration methods, and some specifics about the algorithm in this regard.

## 2 The target theory

We begin our discussion by considering the continuum theory. Our focus will be on the simplest (2,2) 2d WZ model: the one with a cubic superpotential interaction. It is a supersymmetric cousin to an ordinary 2d complex scalar field  $\phi$  model. Two 2d Majorana fermions  $(\psi_-, \bar{\psi}_-)$  and  $(\psi_+, \bar{\psi}_+)$  fit into the same (2,2) supersymmetry multiplet as  $\phi$ .

### 2.1 The action

The Euclidean action that we study is

$$S = \int d^2z \left[ -4\bar{\phi}\partial_z\partial_{\bar{z}}\phi - 2i\bar{\psi}_-\partial_{\bar{z}}\psi_- + 2i\psi_+\partial_z\bar{\psi}_+ - \bar{F}F \right. \\ \left. + W'(\phi)F + \overline{W}'(\bar{\phi})\bar{F} - W''(\phi)\psi_+\psi_- - \overline{W}''(\bar{\phi})\bar{\psi}_-\bar{\psi}_+ \right] \quad (2.1)$$

In these expressions,  $z = x_1 + ix_2 = (\bar{z})^*$ ,  $\partial_z = (\partial_1 - i\partial_2)/2 = (\partial_{\bar{z}})^*$ ,  $d^2z = dz d\bar{z}$ ,  $F$  and  $\phi$  are complex scalar fields,  $W'(\phi) = \partial W/\partial\phi$ , etc., where  $W(\phi)$  is holomorphic in  $\phi$  and is the *superpotential*.  $\psi_{\pm}$  and  $\bar{\psi}_{\pm}$  are independent Grassmann fields: the partition function is  $Z = \int [d^2\phi d^2F d^2\psi_- d^2\psi_+] \exp(-S)$ , where  $d^2\psi_- = d\psi_- d\bar{\psi}_-$ , etc.

Although the quadratic term of the auxiliary field  $F$  has the “wrong” sign, it can be formally integrated by analytic continuation. This allows for the elimination of  $F$ , leading to the action

$$S = \int d^2z \left[ -4\bar{\phi}\partial_z\partial_{\bar{z}}\phi - 2i\bar{\psi}_-\partial_{\bar{z}}\psi_- + 2i\psi_+\partial_z\bar{\psi}_+ \right. \\ \left. + |W'(\phi)|^2 - W''(\phi)\psi_+\psi_- - \overline{W}''(\bar{\phi})\bar{\psi}_-\bar{\psi}_+ \right] \quad (2.2)$$

The continuum partition function is thus  $Z = \int [d^2\phi d^2\psi_- d^2\psi_+] \exp(-S)$ , now with action (2.2).

Of course  $Z$  is at this point only formally defined. Meaning can be assigned to it through perturbation theory about  $\phi = 0$ , or some more general set of classical saddlepoints. In either case, one obtains an asymptotic series that provides approximate results valid in a limited regime. However it is worth noting that the supersymmetry of the model leads to nonrenormalization theorems that allow for a number of exact results to be obtained; see for example [16] and references therein. It is hoped that the lattice formulation that we describe below will give a more complete meaning to the functional integral, outside of perturbation theory and semiclassical expansion. In that case, aspects of the theory that are not protected by nonrenormalization theorems can be studied in a strongly-coupled or deep infrared regime.

We specialize to the superpotential

$$W(\phi) = \frac{m}{2}\phi^2 + \frac{g}{3!}\phi^3 \quad (2.3)$$

Both  $m$  and  $g$  have mass dimension 1. Perturbation theory is defined by  $g/m \ll 1$ . It is useful to make the field redefinition

$$\phi = -\frac{m}{g} + \sigma \quad (2.4)$$

In terms of  $\sigma$ , the superpotential becomes

$$W(\sigma) = -\lambda\sigma + \frac{g}{3!}\sigma^3, \quad \lambda = \frac{m^2}{2g} \quad (2.5)$$

## 2.2 Classical symmetries

With periodic boundary conditions for all fields, the action (2.1) is invariant under the infinitesimal supersymmetry transformations (also true for  $\phi \rightarrow \sigma$ )

$$\begin{aligned} \delta\phi &= \epsilon^- \psi_- + \epsilon^+ \psi_+, & \delta\psi_+ &= -2i\bar{\epsilon}^+ \partial_{\bar{z}}\phi + \epsilon^- F \\ \delta\psi_- &= 2i\bar{\epsilon}^- \partial_z\phi - \epsilon^+ F, & \delta F &= 2i\bar{\epsilon}^- \partial_z\psi_+ + 2i\bar{\epsilon}^+ \partial_{\bar{z}}\psi_- \\ \delta\bar{\phi} &= -\bar{\epsilon}^- \bar{\psi}_- - \bar{\epsilon}^+ \bar{\psi}_+, & \delta\bar{\psi}_+ &= 2i\epsilon^+ \partial_{\bar{z}}\bar{\phi} + \bar{\epsilon}^- \bar{F} \\ \delta\bar{\psi}_- &= -2i\epsilon^- \partial_z\bar{\phi} - \bar{\epsilon}^+ \bar{F}, & \delta\bar{F} &= 2i\epsilon^- \partial_z\bar{\psi}_+ + 2i\epsilon^+ \partial_{\bar{z}}\bar{\psi}_- \end{aligned} \quad (2.6)$$

It can be seen that  $\epsilon^+, \bar{\epsilon}^+$  are associated with  $\partial_{\bar{z}}$  whereas  $\epsilon^-, \bar{\epsilon}^-$  are associated with  $\partial_z$ . We can associate supercharge operators with the transformations (2.6) through

$$\delta \equiv \epsilon^- Q_- + \epsilon^+ Q_+ - \bar{\epsilon}^- \bar{Q}_- - \bar{\epsilon}^+ \bar{Q}_+ \quad (2.7)$$

From this definition it is straightforward to work out the action of  $Q_{\pm}, \bar{Q}_{\pm}$  on the fields. Two subalgebras emerge:

$$\{Q_-, \bar{Q}_-\} = -2i\partial_z, \quad \{Q_+, \bar{Q}_+\} = 2i\partial_{\bar{z}} \quad (2.8)$$

All other anticommutators vanish. Note that from the relation  $t_M = -it_E$  between Minkowski and Euclidean time,

$$z = x + it_E = x - t_M, \quad \bar{z} = x - it_E = x + t_M \quad (2.9)$$

Thus the first subalgebra in (2.8) closes on the generator of left-moving translation and the second subalgebra closes on the generator of right-moving translation. Respectively, there is a left-moving (2,0) algebra and a right-moving (0,2) algebra. The “2” denotes two generators, say  $Q_-$  and  $\bar{Q}_-$ . Taken together, the system has (2,2) supersymmetry.

The superpotential (2.5) has a  $U(1)_R$  symmetry when  $\lambda = 0$ ,  $g \neq 0$  (note that  $\phi = \sigma$  when  $\lambda = 0$ ):

$$\sigma \rightarrow e^{2i\alpha/3}\sigma, \quad \psi_{\pm} \rightarrow e^{-i\alpha/3}\psi_{\pm}, \quad F \rightarrow e^{-4i\alpha/3}F \quad (2.10)$$

and  $\bar{\sigma}, \bar{\psi}_{\pm}, \bar{F}$  transforming as conjugates. Note that  $\sigma$  has R-charge  $2/3$ . Thus  $W \rightarrow \exp(2i\alpha)W$ , which implies that the superpotential (still with  $\lambda = 0$ ) has R-charge 2; this is just the well-known condition to have a  $U(1)_R$  symmetry. That this is an R-symmetry follows from the fact that the component fields of the same supermultiplet have different R-charges, as can be seen from (2.10).

There is also an axial  $U(1)_A$  symmetry that we will make use of:

$$\psi_{\pm} \rightarrow e^{\pm i\omega} \psi_{\pm}, \quad \bar{\psi}_{\pm} \rightarrow e^{\mp i\omega} \bar{\psi}_{\pm} \quad (2.11)$$

with all other fields neutral. Note that this contains fermion parity  $Z_2(F)$  as a subgroup.

We now show that the classical theory with  $\lambda \neq 0$ ,  $g \neq 0$  has an exact  $Z_2(R)$  symmetry. The scalar potential is

$$V = |W'(\sigma)|^2 = \left| \lambda - \frac{g}{2}\sigma^2 \right|^2 \quad (2.12)$$

This potential has minima (recall  $\lambda = m^2/2g$ )

$$\sigma_{\pm} = \pm \sqrt{2\lambda/g} = \pm m/g \quad (2.13)$$

Clearly (2.12) has a  $Z_2$  symmetry  $\sigma \rightarrow -\sigma$  that relates the two classical vacua. The  $Z_2$  is a subgroup of the  $U(1)_R \times U(1)_A$  that survives when  $\lambda \neq 0$  in (2.5), as will be discussed below. Since  $V = |W'(\sigma)|^2 \geq 0$ , these are absolute minima with  $V(\sigma_{\pm}) = 0$ . The saddle point that separates these minima is at the origin, with

$$W''(0) = 0, \quad V(0) = |\lambda|^2 = \frac{|m|^4}{4|g|^2} \quad (2.14)$$

It can be seen that as  $|g|$  is decreased with  $m$  held fixed, the minima separate and the energy density of the barrier between them increases in height.

The effect of  $\lambda \neq 0$  is best understood by treating it as a background field with nonvanishing R-charge. For the superpotential to have the requisite R-charge of 2,  $\lambda$  must have R-charge of  $4/3$ :

$$\lambda \rightarrow e^{4i\alpha/3} \lambda \quad (2.15)$$

Now notice that  $\lambda \neq 0$  is left invariant iff

$$\alpha = \frac{3\pi n}{2}, \quad n \in \mathbf{Z} \quad (2.16)$$

Thus nonzero  $\lambda$  leaves intact the  $Z_4(R)$  subgroup generated by  $\alpha = 3\pi/2$  in Eq. (2.10). At the level of component fields, this transformation is ( $\omega \equiv e^{i\pi/4}$ ):

$$\begin{aligned} \sigma &\rightarrow \Omega(\omega)\sigma = \omega^2\sigma = -\sigma, & \psi_{\pm} &\rightarrow \Omega(\omega)\psi_{\pm} = \omega^{-1}\psi_{\pm} = -i\psi_{\pm} \\ F &\rightarrow \Omega(\omega)F = F \end{aligned} \quad (2.17)$$

and  $\bar{\sigma}, \bar{\psi}_{\pm}, \bar{F}$  transforming as conjugates. Here,  $\Omega$  is the homomorphism that determines how the  $Z_4(R)$  acts on the fields; i.e., their 4-ality. It is easily checked that this is a symmetry of the full action with superpotential (2.5).

To obtain the promised  $Z_2(R)$ , we combine the transformation (2.17) with a  $Z_4(A)$  subgroup of the  $U(1)_A$  that appeared in in (2.11). We describe it by the action of a generator  $\gamma_3$ :

$$\gamma_3 : \quad \psi_+ \rightarrow i\psi_+, \quad \psi_- \rightarrow -i\psi_-, \quad \bar{\psi}_+ \rightarrow -i\bar{\psi}_+, \quad \bar{\psi}_- \rightarrow i\bar{\psi}_- \quad (2.18)$$

The  $Z_2(R)$  is generated by  $\gamma_3\Omega(\omega)$ :

$$Z_2(R) : \quad \sigma \rightarrow -\sigma, \quad \bar{\sigma} \rightarrow -\bar{\sigma}, \quad \psi_{\pm} \rightarrow \pm\psi_{\pm}, \quad \bar{\psi}_{\pm} \rightarrow \pm\bar{\psi}_{\pm} \quad (2.19)$$

Thus for  $\lambda \neq 0, g \neq 0$ , or equivalently  $m \neq 0, g \neq 0$ , the surviving global symmetry is  $U(1)_A \times Z_4(R) \equiv U(1)_A \times Z_2(R)$ .

At infinite volume, the classical  $Z_2(R)$  symmetry must be spontaneously broken. This is because the scalar potential is positive semi-definite:  $V = |W'(\sigma)|^2$ . In this case, the stability of the scalar potential implies in 2d that there are no nontrivial finite action solutions: only the constant absolute minima  $\sigma_{\pm}$  of (2.13) have finite action.<sup>2</sup> Thus instantons do not exist, tunneling does not occur, and the symmetry is spontaneously broken.

## 2.3 Renormalization

The only renormalization of the superpotential  $W$  is that due to wavefunction renormalization [1], with all component fields in the same supermultiplet rescaled identically.<sup>3</sup> Thus if the bare fields and renormalized fields are related by  $\phi = \sqrt{Z}\phi_r$ ,  $\psi_{\pm} = \sqrt{Z}\psi_{\pm,r}$ , etc, then the renormalized superpotential is completely described by the identification  $W(m, g|\phi) \equiv W(m_r, g_r|\phi_r)$  with

$$m_r = Zm, \quad g_r = Z^{3/2}g \quad (2.20)$$

Note that this implies  $\lambda_r = \sqrt{Z}\lambda$ . Counterterms  $\delta m$  and  $\delta g$  for the couplings are not required. I.e., there is no additive renormalization of  $m$  or  $g$ ; if the bare mass  $m = 0$ , then the theory remains massless under renormalization. This can also be seen as a consequence of the  $U(1)_R$  symmetry (2.10) that occurs if  $m = 0$ . Since a continuous symmetry cannot be broken in 2d [12], we know that a mass term cannot be radiatively generated, since that would break the  $U(1)_R$  symmetry. Thus in the continuum theory the critical domain is the neighborhood of  $m = 0$  for any  $g$ . We will find that this is likewise true in the lattice theory.

<sup>2</sup>See for example Section 41.4 of [17].

<sup>3</sup>Of course, Wess and Zumino proved the nonrenormalization theorem in 4d; but the crucial cancellations, due to the 4 conserved supercharges, continue to hold in 2d.

### 3 The lattice action

We now describe the Q-exact lattice action that is the subject of our Monte Carlo simulation studies. The general form of this action was first constructed in [3, 4] using a Nicolai map [5] approach. In [9], Monte Carlo simulations were performed. These demonstrated that Ward identities associated with the (2,2) supersymmetry of the continuum theory were satisfied to such a good approximation that no statistically significant violation could be observed, even with a large sample size. In [8] and [9], two different methods demonstrated boson-fermion spectrum degeneracy for the lightest states, a necessary condition for supersymmetry. Furthermore, the numerical values for the light spectrum agreed with those obtained on the  $Q, Q^\dagger$ -preserving spatial lattice in [3]. In [11] the lattice action was derived using a lattice superfield approach. It was shown how to introduce a Wilson mass term in the superpotential to lift doublers, while keeping the one exact supersymmetry. The same Wilson mass term also appeared in the Nicolai map construction of [3, 4]. In [11] it was shown that in the  $a \rightarrow 0$  limit the lattice perturbation series goes over to that of the continuum without the need for any counterterms, to all orders in the coupling  $g$ .

With auxiliary fields eliminated, and implicit summation over repeated lattice site indices  $m, n$ , the action is:<sup>4</sup>

$$\begin{aligned}
 S = & 4[\Delta_z^S \bar{\phi} + \frac{i}{2} W'(\phi)]_m [\Delta_{\bar{z}}^S \phi - \frac{i}{2} \bar{W}'(\bar{\phi})]_m - 2i \bar{\psi}_{-,m} \Delta_{\bar{z}}^S \psi_{-,m} \\
 & + 2i \psi_{+,m} \Delta_z^S \bar{\psi}_{+,m} - \psi_{+,m} W''(\phi)_{mn} \psi_{-,n} - \bar{\psi}_{-,m} \bar{W}''(\bar{\phi})_{mn} \bar{\psi}_{+,n} \quad (3.1)
 \end{aligned}$$

For convenience, we define the superpotential to include a sum over lattice sites:

$$W = \sum_m \left( -\frac{r}{4} \phi_m \Delta^2 \phi_m + \sum_{n>0} \frac{g_n}{n!} \phi_m^n \right) \quad (3.2)$$

The purpose of the Wilson mass term  $\phi \Delta^2 \phi$ , which includes nearest neighbor interactions, is to lift doublers in the spectrum in a supersymmetric way. From (3.2) one obtains

$$W'(\phi)_m = \frac{\partial W}{\partial \phi_m}, \quad W''(\phi)_{mn} = \frac{\partial^2 W}{\partial \phi_m \partial \phi_n} \quad (3.3)$$

In expressions (3.1) and (3.2), the following finite difference operators are used:

$$\begin{aligned}
 \Delta_\mu^S &= \frac{1}{2} (\Delta_\mu^+ + \Delta_\mu^-), & \Delta^2 &= \sum_{\mu=1,2} \Delta_\mu^+ \Delta_\mu^- \\
 \Delta_z^S &= \frac{1}{2} (\Delta_1^S - i \Delta_2^S), & \Delta_{\bar{z}}^S &= \frac{1}{2} (\Delta_1^S + i \Delta_2^S) \quad (3.4)
 \end{aligned}$$

---

<sup>4</sup>In all of our expressions we work in the natural lattice units  $a = 1$ , unless otherwise noted.

where  $\Delta_\mu^+$  and  $\Delta_\mu^-$  are the usual forward and backward difference operators respectively. From now on we drop the superscript  $S$ , leaving it implied, except on the operator

$$\Delta^{S2} = \sum_\mu \Delta_\mu^S \Delta_\mu^S = 4\Delta_z^S \Delta_{\bar{z}}^S \quad (3.5)$$

which we want to distinguish from  $\Delta^2$ . We will often suppress site indices as well.

We pause to note that (3.1) may be obtained in terms of the one exact lattice supersymmetry  $Q$  acting on an expression of component fields. This  $Q$  is the linear combination  $Q = Q_- + \bar{Q}_+$  of continuum supersymmetries (2.6)-(2.7), with  $\partial_z \rightarrow \Delta_z$  and  $\partial_{\bar{z}} \rightarrow \Delta_{\bar{z}}$ . Note that

$$Q^2 = \frac{1}{2}\{Q_- + \bar{Q}_+, Q_- + \bar{Q}_+\} = 0 \quad (3.6)$$

so that  $Q$  is indeed nilpotent. For reference, the action of  $Q$  on the component fields is

$$\begin{aligned} Q\phi &= \psi_-, & Q\psi_+ &= F + 2i\Delta_{\bar{z}}\phi, & Q\psi_- &= 0, & QF &= -2i\Delta_{\bar{z}}\psi_-, \\ Q\bar{\phi} &= \bar{\psi}_+, & Q\bar{\psi}_+ &= 0, & Q\bar{\psi}_- &= \bar{F} - 2i\Delta_z\bar{\phi}, & Q\bar{F} &= 2i\Delta_z\bar{\psi}_+ \end{aligned} \quad (3.7)$$

from which one can explicitly verify the property (3.6). For a general holomorphic function  $W'_m(\phi)$  we find that

$$\begin{aligned} S &= Q \left( -F\bar{\psi}_- - 2i\psi_+\Delta_z\bar{\phi} + W'(\phi)\psi_+ + \bar{W}'(\bar{\phi})\bar{\psi}_- \right) \\ &= -2i\bar{\psi}_-\Delta_{\bar{z}}\psi_- + 2i\psi_+\Delta_z\bar{\psi}_+ - 4\bar{\phi}\Delta_z\Delta_{\bar{z}}\phi - \bar{F}F - \bar{\psi}_-\bar{W}''\bar{\psi}_+ \\ &\quad - \psi_+W''\psi_- + W'(\phi)(F + 2i\Delta_{\bar{z}}\phi) + \bar{W}'(\bar{\phi})(\bar{F} - 2i\Delta_z\bar{\phi}) \end{aligned} \quad (3.8)$$

Upon elimination of the auxiliary field  $F$  through its equation of motion, (3.8) becomes just the action (3.1).

Because (3.8) is  $Q$ -exact, i.e.,  $S = Q(\dots)$ , we know that  $QS = 0$ . That is, the exact supersymmetric invariance of the lattice action w.r.t.  $Q$  just follows from the nilpotency of  $Q$  and the  $Q$ -exactness of the lattice action. This obviously provides a mechanism by which a host of supersymmetric lattice systems can be constructed. In [11] it was shown that (3.1) is far from the most general action with the symmetries of (3.1). Hence the importance of studying the renormalization of the lattice theory. In particular, we would like to examine whether or not relations like (2.20) hold. In our simulation results below, we will find evidence that (2.20) is approximately true, in a regime where  $a \ll 1$ .

It is a simple matter to specialize to the case of the cubic superpotential. Then

$$W(\phi) = \sum_m \left( -\frac{r}{4}\phi_m\Delta^2\phi_m + \frac{m}{2}\phi_m^2 + \frac{g}{3!}\phi_m^3 \right) \quad (3.9)$$

The action can be written as  $S = S_0 + S_{int}$ , where  $S_0$  is quadratic in fields:

$$\begin{aligned}
S_0 = & \bar{\phi} \left[ -\Delta^{S^2} + (\bar{m} - \frac{\bar{r}}{2}\Delta^2)(m - \frac{r}{2}\Delta^2) \right] \phi - 2i\bar{\psi}_- \Delta_{\bar{z}} \psi_- \\
& + 2i\psi_+ \Delta_z \bar{\psi}_+ - \psi_+(m - \frac{r}{2}\Delta^2)\psi_- - \bar{\psi}_-(\bar{m} - \frac{\bar{r}}{2}\Delta^2)\bar{\psi}_+ \quad (3.10)
\end{aligned}$$

At  $r = 0$  the bosons and fermions both have doublers. The Wilson mass terms at  $r \neq 0$  lifts these modes. Note that the inverse free propagator for the boson is the square of that for the fermions. This is a consequence of the exact lattice supersymmetry, and is a property that is crucial to the perturbative results that were mentioned above. The interaction terms are contained in

$$\begin{aligned}
S_{int} = & -g\phi\psi_+\psi_- - \bar{g}\bar{\phi}\bar{\psi}_-\bar{\psi}_+ + \frac{1}{2}\bar{g}m\bar{\phi}^2\phi + \frac{1}{2}g\bar{m}\phi^2\bar{\phi} + \frac{1}{4}|g|^2\phi^2\bar{\phi}^2 \\
& - \frac{1}{4}r\bar{g}\bar{\phi}^2\Delta^2\phi - \frac{1}{4}\bar{r}g\phi^2\Delta^2\bar{\phi} + ig\phi^2\Delta_{\bar{z}}\phi - i\bar{g}\bar{\phi}^2\Delta_z\bar{\phi} \quad (3.11)
\end{aligned}$$

Note that irrelevant operators appear in the second line. These are a consequence of the exact lattice supersymmetry. The  $r$ -dependent terms originate from the supersymmetrization of the Wilson mass term. The other two arise from crossterms in the first line of (3.1), such as  $W'(\phi)\Delta_{\bar{z}}\phi$ . The crossterms only contribute to interactions, due to the identity  $\phi\Delta_{\mu}^S\phi = 0$  on a periodic lattice.

The irrelevant operators coming from crossterms violate the  $Z_4$  rotation symmetry of the lattice, as well as reflection positivity. As is well-known,  $Z_4$  rotation symmetry is sufficient to imply Euclidean rotation invariance,  $SO(2)$ , of the continuum limit. Thus the violation of  $Z_4$  rotation symmetry is an important matter, since it could conceivably destroy Euclidean invariance of the continuum limit. It can be shown [11] that the  $Z_4$  breaking in this system is an  $\mathcal{O}(a^2g_{phys})$  effect, where  $g_{phys}$  is the coupling in physical units. It is harmless to the continuum limit in perturbation theory, as the lattice perturbation series turns out to be finite. However, it remains to be shown that this does not affect the continuum limit at a nonperturbative level. We will defer detailed discussion of this issue to a later publication. Suffice it to say, we have found in simulations that Green function data at more than a few lattice spacings exhibits approximate  $Z_4$  symmetry, and that this approximation improves as one approaches the continuum limit. As to the lack of reflection positivity, this too is an  $\mathcal{O}(a^2g_{phys})$  effect. Some problems were detected in propagators at  $g_{phys} = \mathcal{O}(1)$  in [9]; however, these difficulties apparently went away for sufficiently small lattice spacing  $a$ . In the studies that we perform here, we work in a regime where  $g = g_{phys}a \ll 1$ , where the violation of reflection positivity by irrelevant operators is believed to be harmless.

Next, consider the field redefinition (2.4) in the lattice theory. One finds

$$W(\sigma) = \sum_m \left( -\frac{r}{4}\sigma_m\Delta^2\sigma_m - \lambda\sigma_m + \frac{g}{3!}\sigma_m^3 \right) \quad (3.12)$$

and the lattice action is just (3.1) with  $\phi \rightarrow \sigma$ . If  $r = 0$ , then  $W'(\sigma)$  is even and  $W''(\sigma)$  is odd under the  $Z_2(R)$  transformation (2.19). Taking into account the

transformation of the fermions, the action is by inspection  $Z_2(R)$  invariant. However, the Wilson mass term violates the  $Z_2(R)$  symmetry (2.19) since for  $r \neq 0$ ,  $W'(\sigma)$  and  $W''(\sigma)$  no longer have definite parity with respect to  $Z_2(R)$ . On the other hand, the symmetry breaking arises entirely from irrelevant higher-derivative terms. Given that the lattice perturbation series is finite, the  $Z_2(R)$  is restored in the continuum limit in perturbation theory. What is left to check is that this occurs nonperturbatively. We will find rather strong evidence that this is true.

Finally, we note that in all of our simulations we set  $r = 1$  in the Wilson mass term.

## 4 Simulation results

### 4.1 Location of the critical domain

First we introduce observables that allow us to locate the critical domain.<sup>5</sup> For a generic choice of the bare parameters  $m$  and  $g$ , the effective potential has two minima, in correspondence with the classical minima  $\sigma_{\pm}$  of (2.13). We will refer to these two minima of the effective potential as the  $\sigma_{\pm}$  vacua, although their location will be somewhat shifted from the classical values. The definitions that we choose are intended to address the following issue related to the existence of two vacua. At finite volume tunneling between the two vacua  $\sigma_{\pm}$  will occur. This is important, because the tunneling events are very large fluctuations, of order  $m/g$ . We do not want to include such fluctuations in the measurement of correlations, since they do not correspond to fluctuations about one of the  $Z_2(R)$  symmetry breaking vacua in the thermodynamic limit. By  $\sigma_{\pm}$  domains we will mean connected regions where  $\sigma$  is closer to one minimum of the effective potential than the other. Several  $\sigma_{\pm}$  domains may establish themselves on the  $N \times N$  lattice, particularly for large  $N$ . In that case what we really want to measure is the fluctuation away from the average value within a domain.

Under the assumption of approximate  $Z_2(R)$  symmetry of the effective potential at finite volume, we expect that the following occurs. Take  $m, g$  real so that the classical minima (2.13) are real. Denote the real and imaginary parts of  $\sigma_m$  as  $\sigma_{R,m}$  and  $\sigma_{I,m}$  respectively. Suppose we have an ensemble of configurations  $\Gamma$ . We partition this ensemble as  $\Gamma = \Gamma_+ + \Gamma_- + \Gamma_0$  where:  $\sigma_{R,m} > 0$  on the subensemble  $\Gamma_+$ ,  $\sigma_{R,m} < 0$  on the subensemble  $\Gamma_-$ , and  $\sigma_{R,m} = 0$  on the subensemble  $\Gamma_0$ . Note that  $\Gamma_0$  is a set of measure zero in any expectation value over  $\Gamma$ , since  $\sigma_{R,m}$  is a continuous variable. Let  $\langle \sigma_R \rangle_+$  be the average of  $\sigma_{R,m}$  over the subensemble  $\Gamma_+$  and  $\langle \sigma_R \rangle_-$  be the average for the subensemble  $\Gamma_-$ . The order parameter  $\langle |\sigma_R| \rangle$  will denote the average of  $|\sigma_{R,m}|$

---

<sup>5</sup>Of course in our analysis we work at finite volume, so all so-called critical behavior is actually pseudocritical. We will not belabor this point in our terminology by appending “pseudo-” to every instance of “critical.”

$N$	$\langle\sigma_R\rangle_+$	$\langle\sigma_R\rangle_-$	$\langle \sigma_R \rangle$
4	3.505(52)	-3.518(52)	3.512(14)
8	3.337(49)	-3.353(48)	3.3456(87)
16	3.342(60)	-3.349(41)	3.3471(45)

Table 1: Comparison of subensemble order parameters to that of the full ensemble, for  $(m, g) = (0.10, 0.03)$ .

over the full ensemble  $\Gamma$ . Then we expect

$$\langle\sigma_R\rangle_+ = -\langle\sigma_R\rangle_- = \langle|\sigma_R|\rangle \equiv v \quad (4.1)$$

to a very good approximation. The veracity of this conjecture is borne out in our simulations. As an example, in Table 1 we show results for the quantities of (4.1) for  $(m, g) = (0.10, 0.03)$  and three different sizes of  $N \times N$  lattice. Similar behavior was observed at other values of  $(m, g, N)$ . This is already good evidence that  $Z_2(R)$  is a symmetry of the effective potential, to within the 1-2% statistical uncertainties of the measurements.

This motivates the following fluctuation analysis. In either  $\sigma_{\pm}$  domain (connected regions where  $\sigma > 0$  or  $\sigma < 0$ ) we define  $\delta\sigma_{R,m}$  by  $|\sigma_{R,m}| \equiv v + \delta\sigma_{R,m}$ . Thus the fluctuation  $\delta\sigma_{R,m}$  is related to the value of  $\sigma_{R,m}$  through

$$\begin{aligned} \sigma_{R,m} &= v + \delta\sigma_{R,m}, & \sigma_{R,m} > 0 \\ \sigma_{R,m} &= -v - \delta\sigma_{R,m}, & \sigma_{R,m} < 0 \end{aligned} \quad (4.2)$$

In either case, the fluctuation is positive if it moves in the direction that is away from the origin  $\sigma_{R,m} = 0$ , relative to  $\pm v$ ; i.e., in the direction that would increase  $|\sigma_{R,m}|$ . This is shown in Fig. 1. In the thermodynamic limit,  $|\delta\sigma_{R,m}| \ll v$  and  $\delta\sigma_{R,m}$  is just a fluctuation about one of the two vacua, which is what we want to study.

Associated with the fluctuation  $\delta\sigma_{R,m}$  one has the following (momentum space) Green function and susceptibility:

$$\tilde{G}_k(\delta\sigma_R) = \frac{1}{V} \langle |\delta\tilde{\sigma}_{R,k}|^2 \rangle, \quad \chi(\delta\sigma_R) = \tilde{G}_0(\delta\sigma_R) \quad (4.3)$$

Here,  $V = N_1 N_2$  on an  $N_1 \times N_2$  lattice (typically we take  $N_1 = N_2 = N$ ) and our convention for the Fourier transform is

$$\delta\tilde{\sigma}_{R,k} = \sum_m \delta\sigma_{R,m} \exp 2\pi i \left( \frac{k_1 m_1}{N_1} + \frac{k_2 m_2}{N_2} \right) \quad (4.4)$$

A rough estimate of the correlation length is the one used in [18]. It involves the ratio of the Green function  $\tilde{G}_k(\delta\sigma_R)$  at  $k = (0, 0)$  to  $k = (1, 0)$ :

$$\xi(\delta\sigma_R) = \left[ \frac{1}{4 \sin^2(\pi/N_1)} \left( \frac{\tilde{G}_{(0,0)}(\delta\sigma_R)}{\tilde{G}_{(1,0)}(\delta\sigma_R)} - 1 \right) \right]^{1/2} \quad (4.5)$$

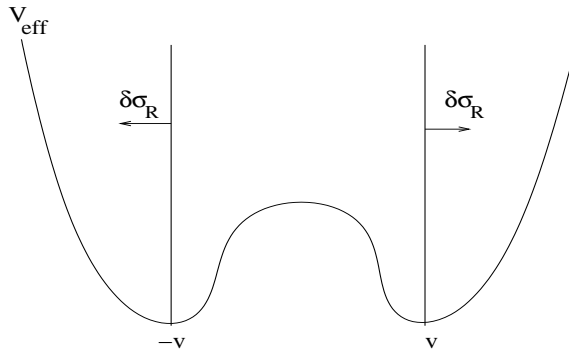


Figure 1: Positive fluctuations  $\delta\sigma_{R,m}$  away from vacua  $\pm v$ .

Near the critical point we expect this quantity to exhibit the correct scaling behavior, at leading order. Since we are not interested in high precision spectral information, (4.5) will suffice for our purpose (determining the location of the critical domain).

We also want to consider fluctuations from the imaginary part of the field  $\sigma$ . Numerically we have found that  $\langle\sigma_{I,m}\rangle = 0$ , for any real  $m, g$ . We therefore define  $\delta\sigma_{I,m} = \sigma_{I,m}$  and

$$\delta\sigma_m = \delta\sigma_{R,m} + i\delta\sigma_{I,m} \quad (4.6)$$

This leads to the Green function  $\tilde{G}_k(\delta\sigma)$ , susceptibility  $\chi(\delta\sigma)$  and correlation length  $\xi(\delta\sigma)$ , obtained through the replacement  $\delta\sigma_R \rightarrow \delta\sigma$  in (4.3),(4.5) above.

In Tables 2-4 we display the measured value for the observables at  $g = 0.03$ , as a function of  $m$ , on three different  $N \times N$  lattices,  $N = 4, 8, 16$ . A value  $g \ll 1$  has been chosen because, as the reader will recall,  $g$  is the coupling in lattice units. Thus in terms of the coupling  $g_{phys}$  in physical units,  $g = g_{phys}a$ . For  $g_{phys} = 1$ , the choice  $g = 0.03$  corresponds to  $a = 0.03$ . Similarly,  $m = m_{phys}a$ , from which one obtains a physical interpretation of the mass.

Several things are to be noted from the data:

- The measured value of  $\langle|\sigma_R|\rangle$  is close to the classical value  $|\sigma_{\pm}| = m/g$  in the case  $g \ll m$ , where perturbation theory applies. Thus the sample is dominated by configurations for which  $\sigma_m$  sits near one of the two classical minima, as one would expect. The classical estimate breaks down as  $m \rightarrow 0$ . Note, however, that if we follow the data at  $m = g$  for  $N = 4, 8, 16$ , the value of  $\langle|\sigma_R|\rangle$  is decreasing, and for  $N = 16$  is only 41% larger than the classical prediction. This implies that for sufficiently large  $N$ , perturbation theory should be trustworthy in the regime  $g/m \lesssim 1$ , as one might guess.
- The  $\delta\sigma_R$  observables of susceptibility and correlation length indicate that the critical domain is in the neighborhood of  $m = 0$ . There is a plateau that is fairly

$m$	$\langle  \sigma_R  \rangle$	$\xi(\delta\sigma_R)$	$\chi(\delta\sigma_R)$	$\xi(\delta\sigma)$	$\chi(\delta\sigma)$
0.00	2.360(30)	7.93(48)	28.8(3.4)	12.51(21)	150.7(4.3)
0.03	2.462(14)	7.86(22)	29.5(1.6)	12.060(93)	139.8(1.9)
0.05	2.624(14)	7.91(23)	29.8(1.7)	11.464(96)	128.1(2.0)
0.10	3.512(14)	7.91(28)	31.2(2.2)	9.23(13)	84.8(2.3)
0.15	5.012(22)	6.68(68)	23.7(4.8)	6.96(35)	48.5(4.8)
0.20	6.6473(89)	4.85(52)	12.8(2.7)	4.89(26)	25.3(2.7)

Table 2: Observables on the  $N = 4$  lattice at  $g = 0.03$ .

$m$	$\langle  \sigma_R  \rangle$	$\xi(\delta\sigma_R)$	$\chi(\delta\sigma_R)$	$\xi(\delta\sigma)$	$\chi(\delta\sigma)$
0.00	1.593(29)	11.6(1.0)	54.3(9.1)	18.30(41)	306(12)
0.03	1.8162(94)	11.08(32)	57.0(3.2)	16.68(14)	262.6(3.8)
0.05	2.0852(99)	11.53(36)	62.3(3.8)	15.13(15)	221.0(4.2)
0.07	2.5037(98)	11.17(41)	61.4(4.4)	13.17(18)	170.6(4.6)
0.10	3.3456(87)	9.72(53)	48.2(5.1)	10.06(25)	103.3(5.2)
0.15	5.0026(60)	7.21(88)	22.7(5.3)	7.17(44)	45.2(5.4)

Table 3: Observables on the  $N = 8$  lattice at  $g = 0.03$ .

$m$	$\langle  \sigma_R  \rangle$	$\xi(\delta\sigma_R)$	$\chi(\delta\sigma_R)$	$\xi(\delta\sigma)$	$\chi(\delta\sigma)$
0.00	1.2261(62)	15.67(49)	98.3(5.9)	25.37(19)	573.7(7.4)
0.01	1.2309(89)	15.93(70)	100.9(8.5)	25.29(27)	564(11)
0.02	1.2802(89)	15.86(71)	102.2(8.8)	24.21(27)	526(11)
0.03	1.4076(66)	16.16(53)	110.9(7.0)	22.73(20)	472.5(8.0)
0.05	1.7818(96)	15.88(86)	116(12)	18.60(37)	330(13)
0.07	2.3579(86)	13.9(1.1)	95(14)	14.56(52)	208(15)
0.10	3.3471(45)	9.9(1.1)	51(11)	9.89(56)	101(11)

Table 4: Observables on the  $N = 16$  lattice at  $g = 0.03$ .

flat (within statistical uncertainties) extending out from  $m = 0$  to some value of  $m$  that is not too large. The range of this plateau appears to be shrinking as  $N$  is increased. From this we conclude that the critical domain shrinks down to an infinitesimal neighborhood of  $m = 0$  in the thermodynamic limit. Note that this is consistent with the nonrenormalization theorem of the continuum theory, expressed by (2.20). That is, if the bare mass  $m$  in (2.20) is set to zero, the renormalized mass  $m_r$  is also zero: there is no additive renormalization. As mentioned above, this can also be viewed as a consequence of the  $U(1)_R$  symmetry, which protects against a mass term in the superpotential. The fact that on the lattice the critical domain is in a shrinking neighborhood of  $m = 0$  leads us to expect that the  $U(1)_R$  symmetry holds to a good approximation for the IR modes in the continuum limit. Further evidence for this will be seen below in Section 4.2.

- There is a hint of a dip in  $\chi(\delta\sigma_R)$  at  $m = 0$ , but the statistical errors are too large to be certain. Simulations at  $m = 0$  are very costly, since the leapfrog evolutions in the hybrid Monte Carlo algorithm become quite unstable, as discussed in Appendix A. In any case, the definition (4.2) of  $\delta\sigma_R$  does not make much sense right at  $m = 0$ , since (at least classically) there is no barrier and the vacuum is unique. At  $m = 0$  it would be more appropriate to study fluctuations of  $\sigma_{R,m}$  rather than  $|\sigma_{R,m}|$ . However, since our purpose here is only to find the critical domain, it is enough to see that the susceptibility  $\chi(\delta\sigma_R)$ , which does make sense at  $m \neq 0$ , is rising as we approach  $m \approx 0$ .
- The  $\delta\sigma$  observables do not show a plateau, but are maximized at  $m = 0$ . The fluctuations  $\delta\sigma_I$  contribute significantly, and in fact dominate, as follows from  $\chi(\delta\sigma) = \chi(\delta\sigma_R) + \chi(\delta\sigma_I)$ . The degree to which this is true increases as we approach  $m = 0$ . We will find further evidence below that  $m = 0$  is the critical point. As a result, the  $\delta\sigma$  observables seem to be better indicators of criticality.

In conclusion, the critical domain is the neighborhood of  $m = 0$ . The continuum renormalization (2.20) appears to hold to a good approximation. At  $m \gg g$ , the theory is noncritical.

## 4.2 R-symmetry of the effective potential

Next we address the two principal questions of this work: (1) To what extent is  $Z_2(R)$  a symmetry of the effective potential? (2) Is  $U(1)_R$  symmetry approximately recovered in the critical domain?

We introduce a complex constant external field  $h$

$$\Delta V(h) = - \sum_m (\bar{h}\sigma_m - h\bar{\sigma}_m) \tag{4.7}$$

to the scalar potential  $V$ . This allows us to explore the effective potential and to study the extent to which it is symmetric w.r.t.  $\sigma \rightarrow -\sigma$ , or the phase rotation  $\sigma \rightarrow e^{i\theta}\sigma$ . As usual, we obtain the effective potential from the Legendre transformation of the generating function  $w(h) = \ln Z(h)$ , where  $Z(h)$  is the partition function that is obtained when (4.7) is added to the lattice action.  $Z_2(R)$  symmetry of the effective potential is equivalent to  $w(-h) = w(h)$ . Similarly,  $U(1)_R$  symmetry of the effective potential is equivalent to  $w(e^{i\theta}h) = w(h)$ . Note also that  $\langle\sigma\rangle_h = \partial w(h)/\partial\bar{h}$ , where  $\langle\sigma\rangle_h$  is the expectation value of  $\sigma$  in the background  $h$ . It follows that in the case of  $Z_2(R)$  symmetry we have the prediction

$$\langle\sigma\rangle_{-h} = -\langle\sigma\rangle_h \quad (4.8)$$

In the case of  $U(1)_R$  symmetry we have the much stronger prediction

$$\langle\sigma\rangle_{e^{i\theta}h} = e^{i\theta}\langle\sigma\rangle_h \quad (4.9)$$

Equivalently, since we take  $m > 0, g > 0$  and will find below that  $\langle\sigma\rangle_h > 0$  if  $h$  is real and positive,

$$\arg\langle\sigma\rangle_h = \arg h, \quad |\langle\sigma\rangle_h| = \text{const.}, \quad \text{fixed } |h| \quad (4.10)$$

is the prediction of  $U(1)_R$  symmetry. The second condition just states that  $|\langle\sigma\rangle_h|^2 = \langle\sigma_R\rangle_h^2 + \langle\sigma_I\rangle_h^2$  is independent of  $\arg h$ .

#### 4.2.1 $Z_2(R)$ tests

Here we consider the case where  $h$  is real. It can be seen from Table 5 that, up to statistical errors, the values of  $\langle\sigma_R\rangle$  are supportive of the  $Z_2(R)$  symmetry prediction (4.8). It is a bit surprising that this is already true on such a small lattice ( $N = 4$ ). Of course  $g/m = 0.15$  is well within the perturbative regime, so upon further reflection it is reasonable that the irrelevant Wilson mass interaction terms that break the  $Z_2(R)$  symmetry would only have a mild influence on the effective potential. Still, it is remarkable that at finite lattice spacing the irrelevant operators have negligible effect.

In Fig. 2 we show the behavior of  $\langle\sigma_R\rangle_h$  on lattices with  $(m, g) = (0.20, 0.03)$  and  $N = 4, 8, 16$ . It can be seen that the transition sharpens significantly as we go from the  $N = 4$  lattice to the  $N = 16$  lattice. Due to nonergodicity in the simulations when the barrier between vacua is large, it was not possible to get stable averages in the transition region, very close to  $h = 0$ , for the  $N = 16$  lattice. So, we have performed a hysteresis study at  $(m, g, N) = (0.20, 0.03, 16)$ .

A simulation was done where a thermalized configuration with  $h = -0.1$  was first produced. Then  $\langle\sigma_R\rangle$  was computed from successive configurations obtain in 20 updates. Next,  $h$  was increased by  $\Delta h = 0.01$ . Then 20 updates were performed and  $\langle\sigma_R\rangle$  was calculated from the 20 configurations that were generated. This was

$ h $	$\langle\sigma_R\rangle(h < 0)$	$\langle\sigma_R\rangle(h > 0)$
0.10	-8.427(19)	8.405(17)
0.01	-6.663(61)	6.7231(45)
0.005	-5.395(56)	5.428(53)
0.003	-3.776(79)	3.897(79)
0.001	-1.408(95)	1.520(98)
0.0005	-0.667(99)	0.694(25)
0.0001	-0.235(96)	0.145(96)
0.0	-0.038(97)	—

Table 5:  $\langle\sigma_R\rangle_h$  as a function of the source  $h$  for  $(m, g, N) = (0.20, 0.03, 4)$ . Note that  $\langle\sigma_I\rangle_h = 0$  for  $h$  real.

continued up to  $h = 0.1$ . Then the cycle was reversed, decreasing  $h$  by the same increment. The results are presented in Fig. 3. It can be seen that there is a pronounced hysteresis. We increased the number of successive configurations at each step of the cycle from 20 to 200 and found that the hysteresis loop did not tighten at all. This is indicative that the transition at  $h \approx 0$  is first order. This is as we should expect from Table 4: the point  $(m, g) = (0.20, 0.03)$  is well outside the critical domain. It is only in the critical domain that the two vacua begin to degenerate, giving rise to the critical fluctuations which occur in a second order transition.

Thus, an interesting question is the extent to which the first order transition softens in the vicinity of the critical domain  $m \approx 0$ . To study this we have produced hysteresis curves like Fig. 3 for a sequence of decreasing  $m$ , holding  $g = 0.03$  fixed. It can be seen that the result is entirely consistent with the conjecture that the critical domain occurs in the neighborhood of  $m = 0$ . The hysteresis curves close up as  $m$  is reduced, indicative of the onset of a second order transition.

Note that the  $h = 0$  data,  $\Delta h > 0$  versus  $\Delta h < 0$ , are closer for  $m = 0$  than for  $m = 0.05$ . This supports the conclusion that  $m = 0$  is the critical point, or the center of the critical domain. From this we draw a conclusion about the plateau and possible dip in  $\delta\sigma_R$  observables that was noted above in relation to Table 4, versus the  $m = 0$  maximum in  $\delta\sigma$  observables, also seen in Table 4. The fact that less hysteresis is observed at  $m = 0$  than at  $m = 0.05$  indicates that the former point is “more critical.” Since the  $\delta\sigma$  observables are noticeably peaked at this point, whereas the  $\delta\sigma_R$  observables are not, we conclude once again that the former observables are better indicators of criticality. Yet more support for these conclusions will be obtained below.

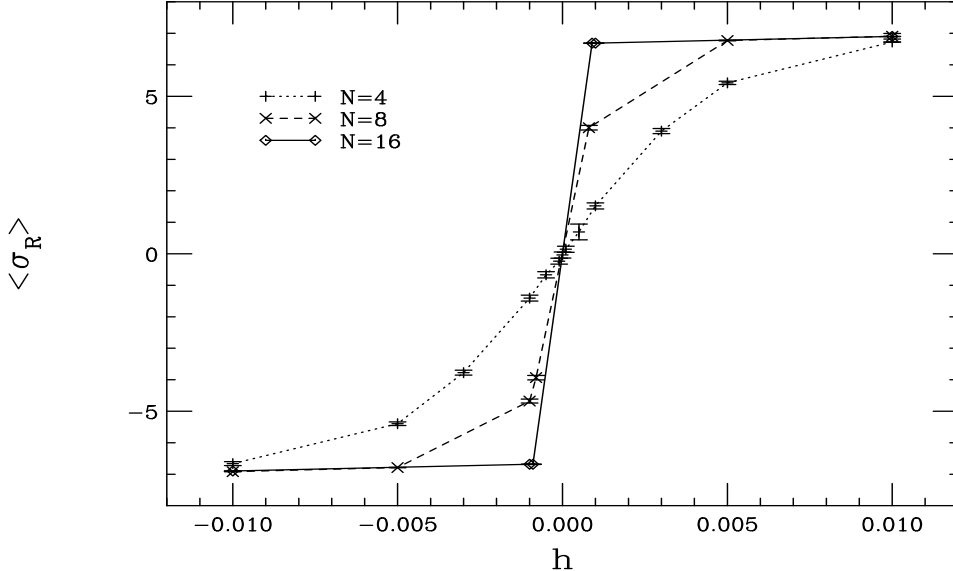


Figure 2:  $\langle \sigma_R \rangle$  versus  $h$  for  $(m, g) = (.20, .03)$ .

#### 4.2.2 $U(1)_R$ tests

Our tests of the  $U(1)_R$  conjecture (4.10) were conducted as follows. Very large ensembles ( $10^4$  independent configurations) were generated at  $(g, h, N) = (0.03, 0, 16)$ , for various values of  $m$ . Expectation values  $\langle \sigma \rangle_h$  at nonzero  $h$  were then obtained by reweighting [19] with the potential (4.7):

$$\langle \sigma \rangle_h = \langle \sigma e^{-\Delta V(h)} \rangle / \langle e^{-\Delta V(h)} \rangle \quad (4.11)$$

The accuracy of the reweighting procedure was verified by comparison to simulations run at a nonzero values of  $h$ . Note that the reweighting (4.11) was not used in the  $Z_2(R)$  tests of Section 4.2.1 above. There, simulations included the potential (4.7). Comparing to expectation values obtained there gives us confidence in the reweighting procedure (4.11).

We keep  $h$  small for three reasons. First, to maintain the reliability of the reweighting procedure, since a large value of  $h$  will tend to lead to overlap problems; i.e., the ensemble of configurations simulated at  $h = 0$  may be distributed very differently from one with a large value of  $h$ . Second, for the  $N = 16$  lattice where we will test for  $U(1)_R$ , the volume  $N^2$  amplifies the effect of  $h$  on the homogeneous mode,  $\tilde{\sigma}_{k=0} = \sum_m \sigma_m$ , whose behavior is characterized by the effective potential. There is already a large sensitivity in  $\langle \sigma \rangle_h = N^{-2} \langle \tilde{\sigma}_{k=0} \rangle$  at very small  $h$ . Third, what we are after are the symmetries of the effective potential in the  $h \rightarrow 0$  limit.

In Fig. 5 we display  $\arg \langle \sigma \rangle_h$  versus  $\arg h$  at  $(g, |h|, N) = (0.03, 0.001, 16)$  for three different mass values,  $m = 0, 0.03, 0.10$ . For  $m = 0$ , the data passes through the

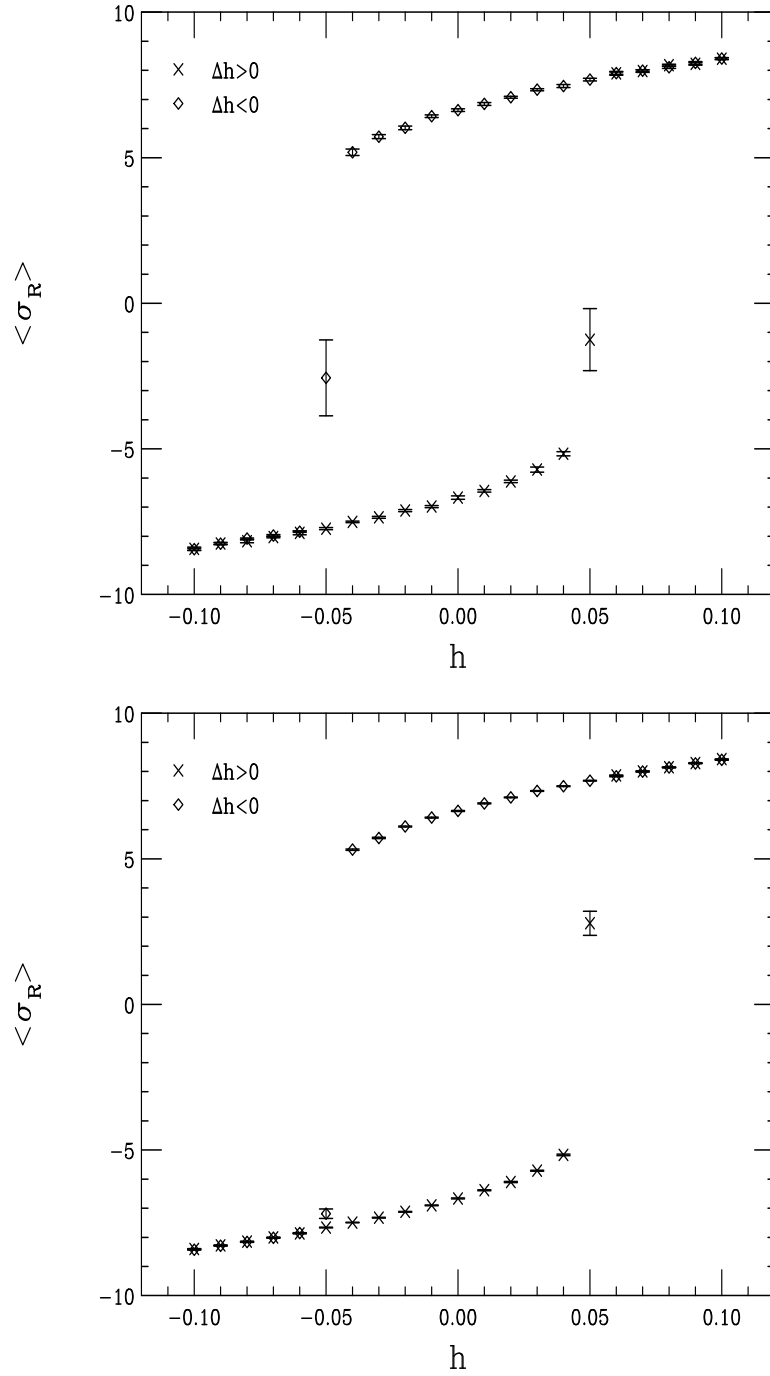


Figure 3: Hysteresis cycles for  $\langle \sigma_R \rangle$  versus  $h$  at  $(m, g, N) = (0.20, 0.03, 16)$ . The top figure had 20 successive configurations at each value of  $h$  along the cycle, whereas the bottom figure had 200.

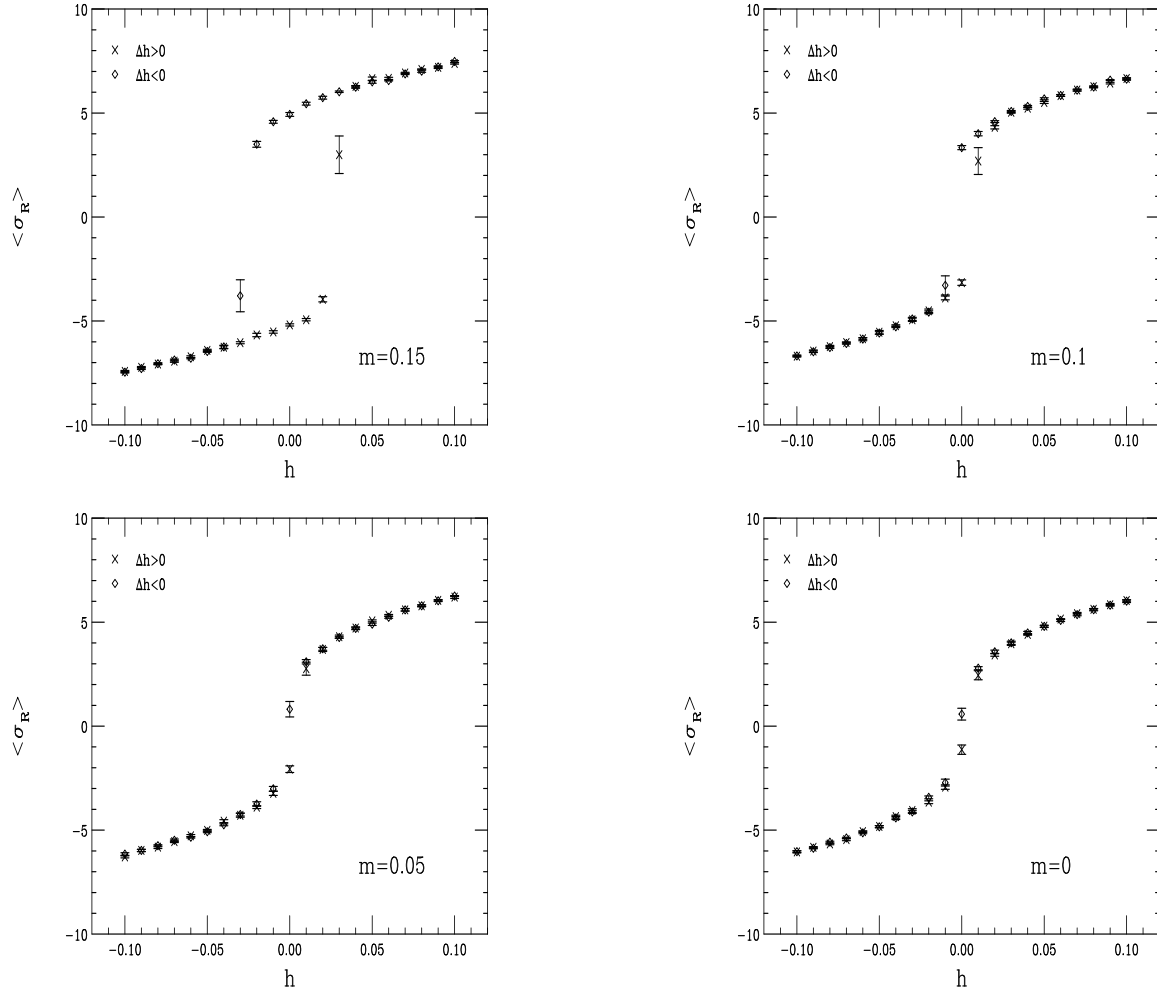


Figure 4: Hysteresis cycles for  $\langle \sigma_R \rangle$  versus  $h$  at  $(g, N) = (0.03, 16)$ , for various values of  $m$ . We averaged over 20 successive configurations at each value of  $h$  along the cycle.

(diagonal) straight line  $\arg \langle \sigma \rangle = \arg h$ , showing that  $U(1)_R$  is a very good symmetry of the effective potential. For  $m = 0.03$ , the data deviates slightly from the straight line, indicating that the symmetry is only slightly violated. Finally, at  $m = 0.10$ , the symmetry is completely broken. The fact that  $\arg \langle \sigma \rangle_h \approx \pm\pi$  in this case can be understood as follows. For larger values of  $m$  and the very small  $h$  that we choose, the potential  $V = |W'(\sigma)|^2$  dominates over the source potential  $\Delta V(h)$  of (4.7). In that case,  $\langle \sigma \rangle_h \approx \pm v$ . Recall that  $v$  was defined by (4.1), without the source potential. Also recall that  $v$  is real for  $m, g$  real, as we choose here. The role of  $h$  then is just as a perturbation to pick the sign of  $\pm v$ . It follows that  $\arg \langle \sigma \rangle_h \approx \pm\pi$ .

The correlation between Fig. 5 and the results of Table 4 is very good: on the plateau where  $\delta\sigma_R$  observables take their critical values, the  $U(1)_R$  symmetry is a good approximation. At the point where the  $\delta\sigma$  observables are maximized, no  $U(1)_R$  symmetry violation can be seen in Fig. 5 above the statistical uncertainty. This indicates that  $m = 0$  is indeed the critical point, and shows that  $\delta\sigma$  observables are well-suited to studying behavior at that point. We again find that any possible dip in the  $\delta\sigma_R$  observables at  $m = 0$  has no significance to the location of the critical point.

The second part of the conjecture (4.10) was studied through the quantity

$$R(|\langle \sigma \rangle_h|) = \frac{|\langle \sigma \rangle_h| - |\overline{\langle \sigma \rangle}|}{|\overline{\langle \sigma \rangle}|}, \quad |\overline{\langle \sigma \rangle}| = \frac{1}{n} \sum_{j=1}^n |\langle \sigma \rangle_{h_j}| \quad (4.12)$$

where  $h_j = |h| \exp(2\pi i j/n)$  corresponds to the values of  $h$  that were used in the data set. Thus,  $R$  measures the relative shift of  $|\langle \sigma \rangle_h|$  away from the mean, where the mean is taken w.r.t.  $\arg h$ . In Fig. 6 it can be seen that significant deviations away from the mean are observed at  $m > 0$ , with the largest occurring for the value  $m = 0.10$ . (The  $R$  test of Fig. 6 turns out to be more sensitive to the  $U(1)_R$  violations at  $m = 0.03$  than the  $\arg \langle \sigma \rangle_h$  vs.  $\arg h$  test of Fig. 5 was.) On the other hand, it can be seen that the  $U(1)_R$  symmetry conjecture (4.10) holds up quite well at  $m = 0$ . Once again,  $m = 0$  is found to be “more critical” than  $m \approx 0.03$ , and the  $\delta\sigma$  observables seem to be better indicators of criticality than the  $\delta\sigma_R$  observables.

In conclusion, the  $U(1)_R$  symmetry of the effective potential is quite robust at  $m = 0$ . To within statistical errors it is not violated. This provides strong evidence that additive renormalization of mass does not occur in the lattice theory in the continuum limit. The violation of the  $U(1)_R$  symmetry in the lattice action at  $m = 0$  due to the Wilson mass term in the superpotential does not appear to impact the renormalization properties of long distance modes.

## 5 Interpretation and future directions

The simulation results that were presented above are quite encouraging for the Q-exact action of the (2,2) 2d Wess-Zumino model. We have found that the R-symmetry of the continuum theory is a property of the effective potential in the lattice theory.

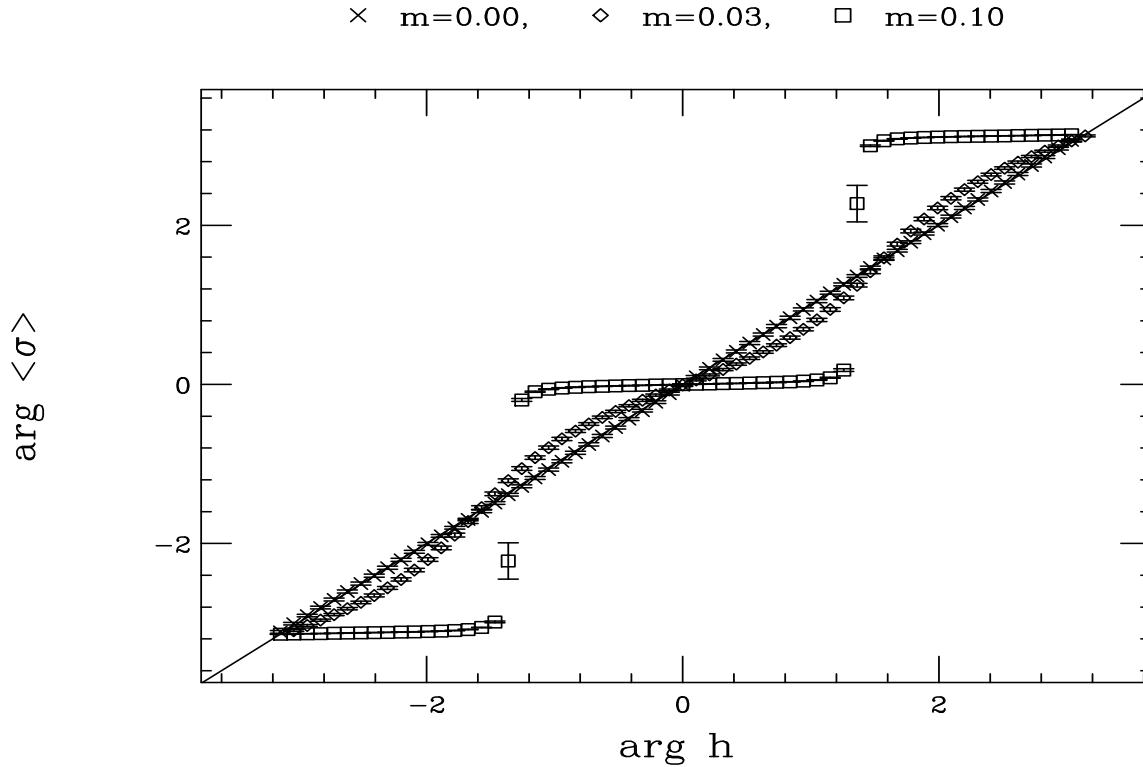


Figure 5: A test of  $U(1)_R$  symmetry, by comparison to the prediction  $\arg \langle \sigma \rangle_h = \arg h$ , indicated by the (diagonal) straight line (mostly hidden by the  $m = 0$  data). It can be seen that the  $m = 0$  data is in very good agreement with the conjecture of  $U(1)_R$  symmetry. At  $m = 0.03$ , where susceptibilities and correlation lengths are close to their critical values, the  $U(1)_R$  symmetry is approximate. At  $m = 0.10$ , where from Table 4 we see that we are certainly outside of the critical domain, the  $U(1)_R$  symmetry is badly broken. This data is for  $(g, |h|, N) = (0.03, 0.001, 16)$ .

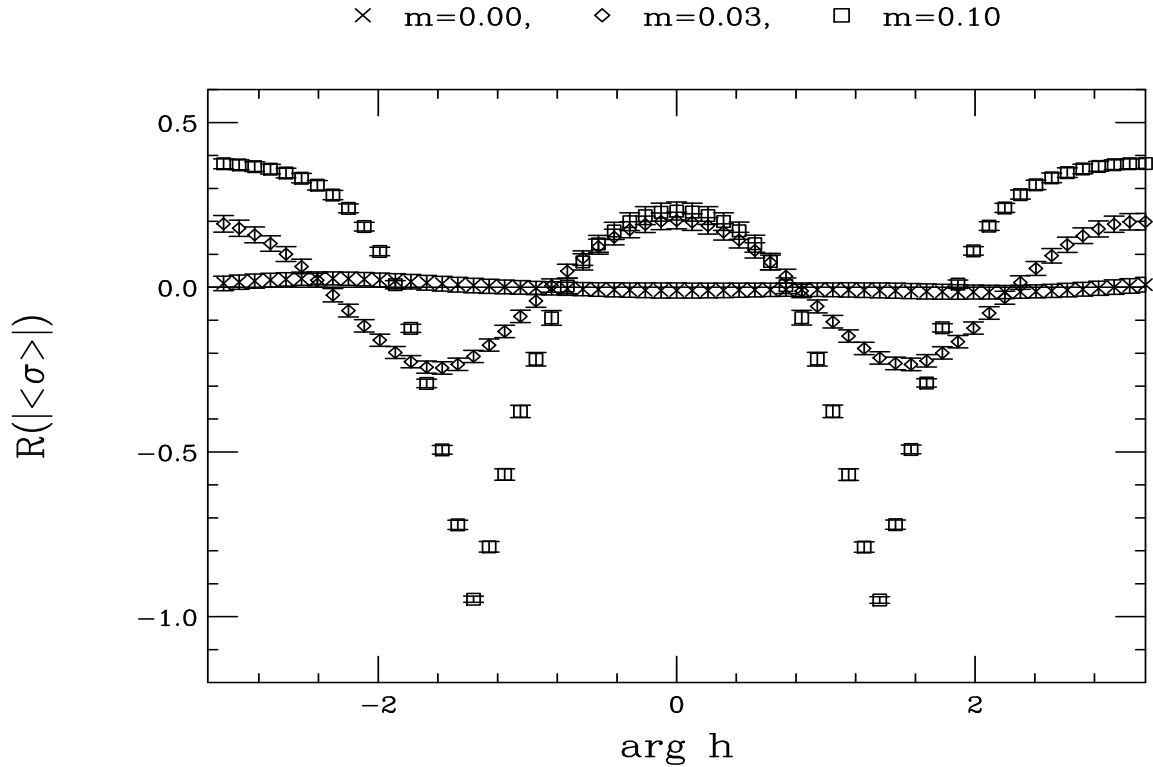


Figure 6: A test of  $U(1)_R$  symmetry, by comparison to the prediction that  $|\langle\sigma\rangle_h|$  should be independent of  $\arg h$ . Relative deviation from the average w.r.t.  $\arg h$  is measured by  $R$  (c.f. eq. (4.12)). The prediction of  $U(1)_R$  symmetry is indicated by the straight line  $R = 0$ . Again, the  $m = 0$  data is in very good agreement with the conjecture of  $U(1)_R$  symmetry,  $m = 0.03$  data indicates that the symmetry is approximate (a maximum of 25% relative violations), whereas  $m = 0.10$  data shows the symmetry is badly broken. This data is for  $(g, |h|, N) = (0.03, 0.001, 16)$ .

The explicit breaking of the R-symmetry due to the Wilson mass term in the superpotential is harmless in the continuum limit; the continuum R-symmetry is recovered without the need for counterterms.

A very important consequence of this is that the nonrenormalization theorems of the continuum theory appear to hold at a nonperturbative level for the long distance modes of the lattice theory. Thus, the good behavior that was already seen to all orders in perturbation theory [11] seems to persist in the strongly coupled regime  $g/m \gtrsim 1$ , where renormalizations are significant. Together with the supersymmetry Ward identity results of [9] and the spectral results of [8, 9], the results presented here provide strong evidence that the nonperturbative physics of the continuum theory can be reliably studied with the Q-exact action. This, in spite of the fact that it only preserves one out of four supercharges and explicitly breaks the R-symmetry, Euclidean invariance, and reflection positivity that are so important to the continuum theory.

Undoubtedly these positive results are related to (i) the fact that the symmetry breaking is due to irrelevant operators and (ii) that 1PI diagrams of UV degree  $D \geq 0$  do not occur in the lattice perturbation series. The cancellations of  $D = 0$  contributions of subdiagrams in lattice perturbation theory is intimately related to the exact lattice supersymmetry [11]. It would be very interesting to know whether or not other lattice actions with an exact supersymmetry, such as the super-Yang-Mills examples that have been recently proposed [13, 20], have a finite lattice perturbation series, in the sense that they have no  $D \geq 0$  1PI diagrams. However, a careful power-counting analysis, comparable to that done by Reisz for 4d Yang-Mills [21], has yet to be performed.<sup>6</sup> If in these lattice super-Yang-Mills theories the perturbation series is finite, the results presented here give some hope that those theories have the correct continuum limit at the nonperturbative level as well.

In research that is in progress, we are currently subjecting the Q-exact lattice system studied here to another nonperturbative test of its continuum limit. As mentioned at the outset, the continuum theory in the critical domain is believed to afford a Landau-Ginzburg description of the minimal discrete series of  $\mathcal{N} = 2$  superconformal field theories. As a result, the critical exponents of all relevant operators are known exactly. If the lattice theory has the correct continuum limit, it should be able to reproduce these exponents. We are presently studying this issue through the examination of hyperscaling (dependence on correlation length) and finite-size scaling (dependence on system size) behavior in the critical regime. We hope to report the results of that study in the near future.

---

<sup>6</sup>As is well-known, the UV behavior of the lattice perturbation series is often worse than the continuum series, due to modified vertices and propagators.

## Acknowledgements

The author would like to thank Erich Poppitz for helpful discussions and comments. Thanks are also due to Simon Catterall and the Syracuse Physics Department for use of their Pentium cluster during some stages of this research. This work was supported by the National Science and Engineering Research Council of Canada and the Ontario Premier's Research Excellence Award.

## Appendix

### A Simulation details

In our simulations, we want to study the behavior of the theory in the critical domain. However, in that case Monte Carlo simulations tend to exhibit critical slowing-down due to long wavelength modes that do not efficiently decorrelate. The characteristic autocorrelation time  $\tau_{AC}$  in simulations grows like

$$\tau_{AC} \sim |m - m_*|^{-z_m} |g - g_*|^{-z_g}, \quad z_m, z_g = \mathcal{O}(1) \quad (\text{A.1})$$

as we approach a critical point  $(m_*, g_*)$ . This is a consequence of the local trajectories through configuration space that a typical simulation method uses. In some systems, global moves [22] based on percolation algorithms [23] can be engineered to completely overcome this problem. For example, in scalar field theories with a  $Z_2$  symmetry one can exploit cluster algorithms that have been developed for the Ising model [22, 24]. Such a global method is not known for the present system.<sup>7</sup> Instead, we have used the method of *Fourier acceleration* [25], as applied [26, 27] to the *hybrid Monte Carlo* (HMC) algorithm [28]. With Fourier acceleration, different Fourier modes are evolved with disproportionate time steps during the *leapfrog* trajectories of the HMC algorithm. This allows the longest wavelength modes to be displaced farther through configuration space, speeding up their decorrelation. Simultaneously, shorter wavelength modes are displaced less far. This keeps acceptance rates in the Metropolis step of HMC high.

We have found that Fourier acceleration significantly reduces autocorrelation times for the present system, as previously noted by Catterall et al. [9]. At points where we have compared the performance of conventional leapfrog to Fourier accelerated leapfrog, we find a reduction of autocorrelation times by an order of magnitude or more. Furthermore, with Fourier acceleration applied to our simulations, we did not

---

<sup>7</sup>It is possible that one might be able to exploit the approximate  $Z_2(R)$  symmetry of the effective potential that is present in this lattice model. A percolation method based on this  $Z_2(R)$  might work well as a *suggestor* algorithm for Metropolis steps. I.e., a percolation method could be used to suggest new configurations, which would be accepted or rejected with a Metropolis criterion.

encounter problems with critical slowing-down. (However, see the discussion below regarding leapfrog integrator instabilities in the critical domain.)

In Eq. (D.16) of [11] it was shown how to write the fermion matrix in a basis where it is real. Once this is done, we can introduce real pseudofermions  $y_{i,\mathbf{m}}$ ,  $i = 1, 2$  to reproduce the fermion determinant:

$$S_P = \frac{1}{2} y^T (M^T M)^{-1} y \quad (\text{A.2})$$

The pseudofermion representation permits HMC simulation of the system. We introduce momenta  $p$  and  $\pi$ , conjugate to  $\phi$  and  $y$  resp., and an auxiliary Hamiltonian:

$$H = \bar{p}p + \frac{1}{2}\pi^2 + S_B + S_P \quad (\text{A.3})$$

With Fourier acceleration, the HMC algorithm invokes molecular dynamics trajectories that evolve the system according to a modified version of Hamilton's equations. The net effect is that the leapfrog steps are done in Fourier space, with each mode evolved with its own molecular dynamics time step. For further details, see the discussion in [27].

After the random update of the conjugate momenta that occurs prior to each molecular dynamics trajectory, we evolve the Fourier modes, labeled by  $k$ , for  $T$  time steps of spacing  $dt_k$ . Thus there is a molecular dynamics evolution for simulation time  $\tau_k = T \cdot dt_k$  between each randomization of the momenta. The Fourier acceleration occurs by choosing  $dt_k \propto 1/\omega_k$ , where  $\omega_k$  is determined by the frequency of modes in the  $g \rightarrow 0$  limit, with some effective *accelerator mass*  $m_{acc}$ , as described in [27]. Although the random updates of the momenta introduce noise, in a generalization of the discrete Langevin equation (see for instance the very nice discussion in [29]), it is still possible that some modes may not decorrelate (over reasonable periods of simulation time). This is due to the coincidences pointed out by Mackenzie [30]. To overcome this potential problem,  $dt$  was randomized. We effect this in the following way. For a given number of steps  $T$ , we choose  $dt_{max}$  such that  $T \cdot dt_{max} = \pi/2$ . We then randomize  $dt$  uniformly in  $(0, dt_{max})$ . The time step for each mode is then determined by  $dt_k = dt/\omega_k$ . This time step is used for the entire molecular dynamics trajectory of  $T$  steps. This algorithm is motivated by the observation [29] that in the  $g = 0$  theory it can be shown that the autocorrelation of a mode  $k$  is proportional to  $\cos_T(T dt_k \omega_k)$ , where  $\cos_T$  is an approximation to cosine that becomes exact as  $T \rightarrow \infty$ . Thus by choosing  $T dt_k \omega_k = \pi/2$  we get almost complete decorrelation in the  $g/m \ll 1$  regime. In our simulations we find rapid decorrelation outside of this regime as well.

We have measured autocorrelation times throughout all of our simulations. We find that

$$\tau_{AC} = \mathcal{O}(1) \times T \quad (\text{A.4})$$

That is, a few hybrid molecular dynamics trajectories are sufficient to decorrelate the configurations. (Hybrid refers to the randomization of momenta prior to each trajectory.) Non-ergodicities were excluded by verifying that measured quantities were independent of initial conditions, and that subensembles gave identical results, within statistical uncertainties.

Unfortunately, as we approach the critical point  $m = 0$ , the number of steps  $T$  in the leapfrog evolution must typically be chosen very large. Recall that  $Tdt_{max}$  is held fixed. If  $dt_{max}$  is too large, we find that the leapfrog integrator can become unstable [31, 32]. Thus in practice we choose  $dt_{max}$  as large as leapfrog stability will allow, and adjust  $T$  such that  $Tdt_{max} = \pi/2$ . In the critical domain, acceptance rates are then found to be nearly 100 percent. (Therefore the only purpose of the Metropolis step of HMC is to keep the algorithm “perfect.”) In practice we find that at or near  $m = 0$ , it is necessary to have  $T = \mathcal{O}(10^3)$ . Thus if simulation time is measured in units of  $dt_{max}$ , we do not escape critical slowing down; this is because  $dt_{max}$  must be drastically reduced as the degree of criticality (measured, say, by the correlation length in units of lattice spacing) is increased. A significant speed-up in the simulations could presumably be achieved through the multi-pseudofermion methods discussed in [32].

## References

- [1] J. Wess and B. Zumino, “A Lagrangian Model Invariant Under Supergauge Transformations,” *Phys. Lett. B* **49** (1974) 52.
- [2] W. Boucher, D. Friedan and A. Kent, “Determinant Formulae And Unitarity For The N=2 Superconformal Algebras In Two-Dimensions Or Exact Results On String Compactification,” *Phys. Lett. B* **172**, 316 (1986); P. Di Vecchia, J. L. Petersen, M. Yu and H. B. Zheng, “Explicit Construction Of Unitary Representations Of The N=2 Superconformal Algebra,” *Phys. Lett. B* **174**, 280 (1986).
- [3] S. Elitzur and A. Schwimmer, “N=2 Two-Dimensional Wess-Zumino Model On The Lattice,” *Nucl. Phys. B* **226**, 109 (1983).
- [4] N. Sakai and M. Sakamoto, “Lattice Supersymmetry And The Nicolai Mapping,” *Nucl. Phys. B* **229**, 173 (1983).
- [5] H. Nicolai, “On A New Characterization Of Scalar Supersymmetric Theories,” *Phys. Lett. B* **89** (1980) 341.
- [6] S. Elitzur, E. Rabinovici and A. Schwimmer, “Supersymmetric Models On The Lattice,” *Phys. Lett. B* **119** (1982) 165.

- [7] S. Cecotti and L. Girardello, “Stochastic Processes In Lattice (Extended) Supersymmetry,” Nucl. Phys. B **226**, 417 (1983).
- [8] M. Beccaria, G. Curci and E. D’Ambrosio, “Simulation of supersymmetric models with a local Nicolai map,” Phys. Rev. D **58** (1998) 065009 [arXiv:hep-lat/9804010].
- [9] S. Catterall and S. Karamov, “A two-dimensional lattice model with exact supersymmetry,” Nucl. Phys. Proc. Suppl. **106** (2002) 935 [arXiv:hep-lat/0110071]; S. Catterall and S. Karamov, “Exact lattice supersymmetry: the two-dimensional  $N = 2$  Wess-Zumino model,” Phys. Rev. D **65** (2002) 094501 [arXiv:hep-lat/0108024].
- [10] S. Catterall, “Lattice supersymmetry and topological field theory,” Nucl. Phys. Proc. Suppl. **129** (2004) 871 [arXiv:hep-lat/0309040]; “Lattice supersymmetry and topological field theory,” JHEP **0305** (2003) 038 [arXiv:hep-lat/0301028].
- [11] J. Giedt and E. Poppitz, “Lattice supersymmetry, superfields and renormalization,” JHEP **0409**, 029 (2004) [arXiv:hep-th/0407135].
- [12] N. D. Mermin and H. Wagner, “Absence Of Ferromagnetism Or Antiferromagnetism In One-Dimensional Or Two-Dimensional Isotropic Heisenberg Models,” Phys. Rev. Lett. **17** (1966) 1133; S. R. Coleman, “There Are No Goldstone Bosons In Two-Dimensions,” Commun. Math. Phys. **31** (1973) 259.
- [13] A. G. Cohen, D. B. Kaplan, E. Katz and M. Unsal, “Supersymmetry on a Euclidean spacetime lattice. I: A target theory with four supercharges,” JHEP **0308**, 024 (2003) [arXiv:hep-lat/0302017]; “Supersymmetry on a Euclidean spacetime lattice. II: Target theories with eight supercharges,” JHEP **0312**, 031 (2003) [arXiv:hep-lat/0307012]; D. B. Kaplan and M. Unsal, “A Euclidean lattice construction of supersymmetric Yang-Mills theories with sixteen supercharges,” arXiv:hep-lat/0503039; F. Sugino, “A lattice formulation of super Yang-Mills theories with exact supersymmetry,” JHEP **0401** (2004) 015 [arXiv:hep-lat/0311021]; “Super Yang-Mills theories on the two-dimensional lattice with exact supersymmetry,” JHEP **0403** (2004) 067 [arXiv:hep-lat/0401017]; “Various super Yang-Mills theories with exact supersymmetry on the lattice,” JHEP **0501** (2005) 016 [arXiv:hep-lat/0410035].
- [14] J. Giedt, “Non-positive fermion determinants in lattice supersymmetry,” Nucl. Phys. B **668** (2003) 138 [arXiv:hep-lat/0304006]; “The fermion determinant in (4,4) 2d lattice super-Yang-Mills,” Nucl. Phys. B **674** (2003) 259 [arXiv:hep-lat/0307024].
- [15] J. Giedt, “Deconstruction, 2d lattice super-Yang-Mills, and the dynamical lattice spacing,” arXiv:hep-lat/0405021.

- [16] E. Witten, “On the Landau-Ginzburg description of N=2 minimal models,” *Int. J. Mod. Phys. A* **9**, 4783 (1994) [arXiv:hep-th/9304026].
- [17] J. Zinn-Justin, “Quantum field theory and critical phenomena,” Fourth Edition, Oxford University Press, Oxford, 2002.
- [18] S. Caracciolo, R. G. Edwards, S. J. Ferreira, A. Pelissetto and A. D. Sokal, “Finite size scaling at  $\xi/L$  much larger than 1,” *Phys. Rev. Lett.* **74** (1995) 2969 [arXiv:hep-lat/9409004].
- [19] M. Falcioni, E. Marinari, M. L. Paciello, G. Parisi and B. Taglienti, “Complex Zeros In The Partition Function Of The Four-Dimensional SU(2) Lattice Gauge Model,” *Phys. Lett. B* **108**, 331 (1982); A. M. Ferrenberg and R. H. Swendsen, “New Monte Carlo Technique For Studying Phase Transitions,” *Phys. Rev. Lett.* **61**, 2635 (1988); “Optimized Monte Carlo Analysis,” *Phys. Rev. Lett.* **63**, 1195 (1989).
- [20] S. Catterall, “A geometrical approach to N = 2 super Yang-Mills theory on the two dimensional lattice,” *JHEP* **0411** (2004) 006 [arXiv:hep-lat/0410052]; “Lattice formulation of N = 4 super Yang-Mills theory,” arXiv:hep-lat/0503036.
- [21] T. Reisz, “Lattice Gauge Theory: Renormalization To All Orders In The Loop Expansion,” *Nucl. Phys. B* **318** (1989) 417.
- [22] R. H. Swendsen and J. S. Wang, “Nonuniversal Critical Dynamics In Monte Carlo Simulations,” *Phys. Rev. Lett.* **58**, 86 (1987).
- [23] P. W. Kasteleyn and C. M. Fortuin, *J. Phys. Soc. Jpn. Suppl.* **26s**, 11 (1969); C. M. Fortuin and P. W. Kasteleyn, “On The Random Cluster Model. 1. Introduction And Relation To Other Models,” *Physica* **57**, 536 (1972).
- [24] I. Montvay and P. Weisz, “Numerical Study Of Finite Volume Effects In The Four-Dimensional Ising Model,” *Nucl. Phys. B* **290**, 327 (1987); U. Wolff, “Lattice Field Theory As A Percolation Process,” *Phys. Rev. Lett.* **60**, 1461 (1988).
- [25] C. Davies *et al.*, “Langevin Simulations Of Lattice Field Theories Using Fourier Acceleration,” *J. Statist. Phys.* **43**, 1073 (1986); C. T. H. Davies *et al.*, “Fourier Acceleration In Lattice Gauge Theories. 1. Landau Gauge Fixing,” *Phys. Rev. D* **37**, 1581 (1988); G. Katz *et al.*, “Fourier Acceleration. 2. Matrix Inversion And The Quark Propagator,” *Phys. Rev. D* **37**, 1589 (1988).
- [26] S. Catterall and E. Gregory, “A lattice path integral for supersymmetric quantum mechanics,” *Phys. Lett. B* **487**, 349 (2000) [arXiv:hep-lat/0006013].
- [27] S. Catterall and S. Karamov, “Testing a Fourier accelerated hybrid Monte Carlo algorithm,” *Phys. Lett. B* **528**, 301 (2002) [arXiv:hep-lat/0112025].

- [28] S. Duane, A. D. Kennedy, B. J. Pendleton and D. Roweth, “Hybrid Monte Carlo,” *Phys. Lett. B* **195**, 216 (1987).
- [29] A. S. Kronfeld, “Dynamics of Langevin simulations,” *Prog. Theor. Phys. Suppl.* **111**, 293 (1993) [arXiv:hep-lat/9205008].
- [30] P. B. Mackenzie, “An Improved Hybrid Monte Carlo Method,” *Phys. Lett. B* **226**, 369 (1989).
- [31] B. Joo, B. Pendleton, A. D. Kennedy, A. C. Irving, J. C. Sexton, S. M. Pickles and S. P. Booth [UKQCD Collaboration], “Instability in the molecular dynamics step of hybrid Monte Carlo in dynamical fermion lattice QCD simulations,” *Phys. Rev. D* **62**, 114501 (2000) [arXiv:hep-lat/0005023].
- [32] A. D. Kennedy, “Algorithms for lattice QCD with dynamical fermions,” *Nucl. Phys. Proc. Suppl.* **140**, 190 (2005) [arXiv:hep-lat/0409167].